SUPERSONIC imagine

The Theragnostic Company™

SuperSonic Imagine, S.A.
Les Jardins de la Duranne - Bât. F
510 rue René Descartes
Aix-en-Provence, Cedex 13857
France
Phone : +33 442 99 24 24
Fax: +33 442 52 59 21

SuperSonic Imagine Inc.
8347 154th Ave NE
Redmond, WA 98052
Phone: +1 (425) 284-6610
Fax: +1 (425) 284-6623
USA

SuperSonic Imagine Ltd.
18 Upper Walk
Virginia Water
Surrey GU25 4SN
Phone: +44 (0) 845 643-4516
UNITED KINGDOM

SuperSonic Imagine GmbH
Dietlindenstraße 15
80802 München
Phone: +49 89 36036 884
Fax: +49 160 94 669 144
GERMANY

SuperSonic Imagine

27V1-MI2D081118B11

VISUALSONICS

White Paper:

Photoacoustic Imaging of Murine Tumors Using the Vevo® 2100 Micro-Ultrasound System

Ver 1.0

Table of Contents

Summary

The VisualSonics Vevo 2100 linear array system offers a selection of imaging modalities that have been recently enhanced by the addition of photoacoustic capabilities. A preclinical model of subcutaneous tumors has been investigated using various imaging techniques, including B-Mode ultrasound, Power Doppler (PD) ultrasound and Photoacoustics (PA). PD is a conventional ultrasound imaging technique which indicates the presence of blood flow within soft tissues. B-Mode and PD images are compared with new PA parametric images of hemoglobin concentration and oxygen saturation. These various imaging modes on the Vevo 2100 micro-ultrasound system, which can all be co-registered to the same image plane, allow a variety of measurements to be carried across modalities and provide inherent fusion of complementary information. The researcher is provided with both structural and physiological information to better understand the biological models at hand.

Introduction

PA Imaging is a method for obtaining optical contrast from biological tissues and detecting it with ultrasound (Oraevsky and Karabutov 2003). By illuminating tissue, a thermoelastic expansion occurs (dependent on optical absorption at the excitation wavelength of the light). This expansion creates an ultrasound wave which can be detected with an ultrasound transducer. PA imaging for biomedical applications has seen tremendous growth in the last decade, with its main applications in cancer research (Siphanto et al. 2005, Zhang et al. 2006, Lungu et al. 2007, Xiang et al. 2007, Ermilov et al. 2009) and brain imaging (Wang et al. 2003, Wang et al. 2008, Laufer et al. 2009). The main advantage of PA is that the optical contrast is combined with the spatial resolution and tissue penetration of ultrasound. Therefore light-absorbing structures deep inside tissues can be detected and visualized with resolutions far superior to pure optical methods (Wang and Wu, 2007). Since light is a non-ionizing electromagnetic wave, PA imaging is considered safe, provided that the optical power is kept within safety limits to avoid thermal or chemical damage to the tissue. The modern realization of the PA effect in biomedical applications involves a short laser pulse irradiating the tissue and ultrasound detection of the PA waves at multiple viewing angles outside the tissue.

The most commonly accepted PA scanners use either a tomographic geometry called PAT (scanning around the subject, similar to x-ray CT) (Xu and Wang 2006) or a planar geometry, using a linear transducer array (Kruger et al. 2003, Zeng et al. 2004). The tomographic approach offers a large effective aperture for data collection, but suffers from a very low frame rate (>10 minutes per 2D frame), due to the need for hundreds to thousands of laser pulses per frame. The use of a linear array (such as offered by VisualSonics) relieves the need for scanning and thus a 2D frame can be acquired with just a few laser pulses, providing much higher frame rates.
PA imaging is well suited to small animal imaging. The length scales involved fit well with the penetration of light into tissue and with the sub-mm image resolution. The resolution is scalable with the frequency of the ultrasound detected. Recently, VisualSonics launched the Vevo 2100 linear array based micro-ultrasound imaging system (Foster et al. 2009). It has a fully developed, 64 channel, high-frequency

VISUALSONICS

beamformer, capable of driving linear arrays in the 12-70 MHz range. VisualSonics has developed a prototype PA imaging system based on linear array technology of the Vevo 2100 system. This enables the collection of both ultrasound and PA images of the same plane, such that they are co-registered and can be overlaid. This is a considerable advantage, since PAT images typically do not convey much anatomical information and thus their interpretation can benefit from the structural information of ultrasound.
In this study the ability of VisualSonics' prototype PA system to image subcutaneous murine tumors was investigated. An emphasis was placed on imaging the vasculature and microvasculature of the tumor, as well as generating parametric maps of physiological significance, namely of hemoglobin concentration and oxygen saturation. Comparison of the PA images with the co-registered B-Mode and PD ultrasound was performed to demonstrate the future potential of PA imaging for pre-clinical research.

Photoacoustic Imaging on the Vevo 2100 System

The PA implementation is depicted in Fig. 1. Light from the laser (OPO pumped by doubled Nd:YAG, tunable 680-950 nm, 20 Hz repetition rate, 5 ns pulse width, 50 mJ pulse energy), was delivered to the tissue through a fiber bundle, split into two rectangular light bars and mounted on each side of the transducer array (MS-250, 21 MHz center frequency). PA waves propagated back to the transducer, coupled through ultrasound gel and were acquired by the transducer array.

Parallel acquisition was used for image formation. In this mode, for each laser pulse, the PA signals were captured on a quadrant of the MS250 array (64 elements). Once all quadrants were acquired, the full dataset was used to beamform an image using a delay and sum algorithm, on dedicated PC software. Since four pulses were required for each image, the frame rate was one fourth of the laser repetition rate (i.e. 5 Hz). 3D PA imaging was performed by scanning the transducer with a linear stepper motor while capturing 2D images.

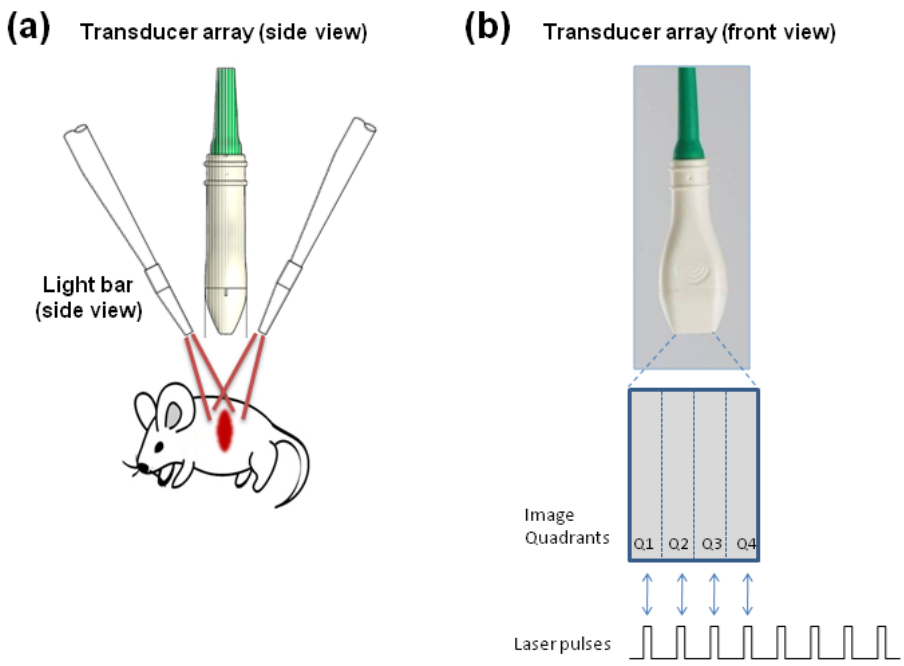

Figure 1: Implementation of the Vevo 2100 PA system. (a) Layout of light delivery and ultrasound detection. Laser light is delivered through rectangular bundles, shown here from the side. The length of the "light bars" was set to equal the length of the array. Ultrasound gel was used in the space between the transducer and skin, in order to couple the PA waves from the tissue to the transducer. (b) Sequence of image acquisition in Parallel mode: For each laser pulse, one quadrant of the transducer array (64 channels) is read out and saved. Once all quadrants are read (4 laser pulses), the data is beamformed to create an image.

The process of 3D acquisition was repeated at several wavelengths, and then parametric maps of hemoglobin concentration and oxygen saturation were calculated, based on a two-wavelength approach (Wang et al. 2006):

$$\mu_a^{\lambda 1}(r) = \frac{P^{\lambda 1}(r)}{\Gamma \cdot F^{\lambda 1}(r)}$$

$$\mu_a^{\lambda 2}(r) = \frac{P^{\lambda 2}(r)}{\Gamma \cdot F^{\lambda 2}(r)}$$

$$HbT(r) = \frac{a_1 \mu_a^{\lambda 1}(r) - a_2 \mu_a^{\lambda 2}(r)}{a_3}$$

$$StO_2(r) = \frac{a_4 \mu_a^{\lambda 2}(r) - a_5 \mu_a^{\lambda 1}(r)}{a_6 \mu_a^{\lambda 1}(r) - a_7 \mu_a^{\lambda 2}(r)}$$

Where P(**r**) was the detected pressure at point **r**, Γ the Gruneisen parameter was 0.1-0.2 in soft tissue, F(**r**) was the estimated fluence of the excitation light, and μ_a(**r**) was the calculated absorption coefficient. The superscripts λ_1 or λ_2 indicate the first or second wavelengths of light used for the measurement. Once the absorption coefficients were determined, the total hemoglobin concentration (HbT) and oxygen saturation (SO_2) could be calculated. The parameters a_1 to a_7 were functions of the extinction coefficients of oxygenated and deoxygenated hemoglobin (see Wang et al. 2006 for detailed expressions). Fig. 2 presents the literature values for the absorption coefficients of hemoglobin at physiological concentrations.

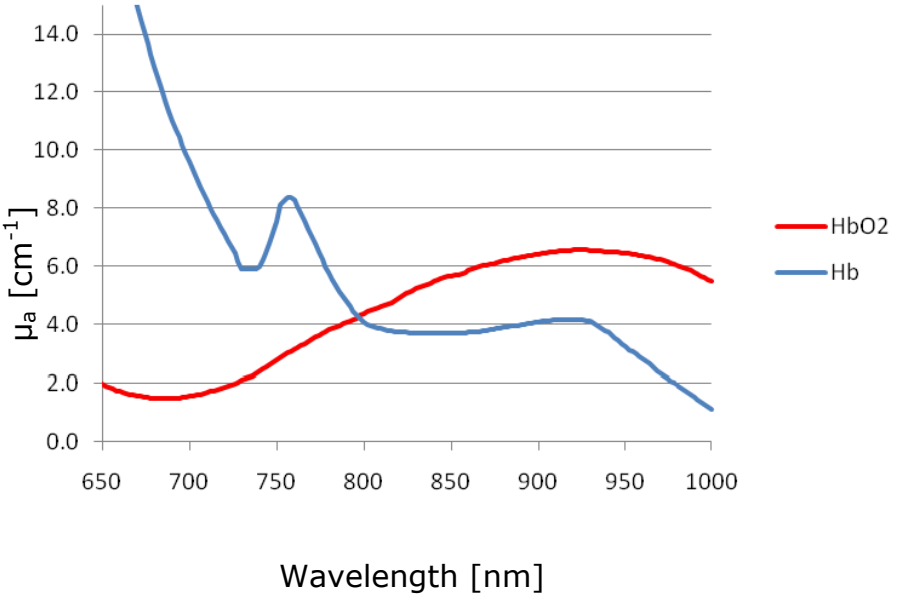

Figure 2: Absorption spectrum of hemoglobin in the spectral range relevant to the VisualSonics laser system (adapted from Prahl 1999). Hb indicates fully deoxygenated hemoglobin, and HbO_2 is 100% oxygenated hemoglobin.

Results

Oxygenation Validation

Fig. 3 presents two maps of oxygenation saturation (SO_2) of a tube filled with venous blood drawn from the tail vein of a mouse. On the left, the blood was drawn after the mouse inhaled anesthetics mixed with room air. The oxygenation is in the range of 50-75%. On the right, the blood was drawn after the mouse inhaled anesthetics mixed with 100% oxygen for 10 minutes. The oxygenation increased significantly to the 95% range. This preliminary experiment demonstrates the ability of Vevo 2100 system to track changes in the oxygenation saturation of blood using PA imaging.

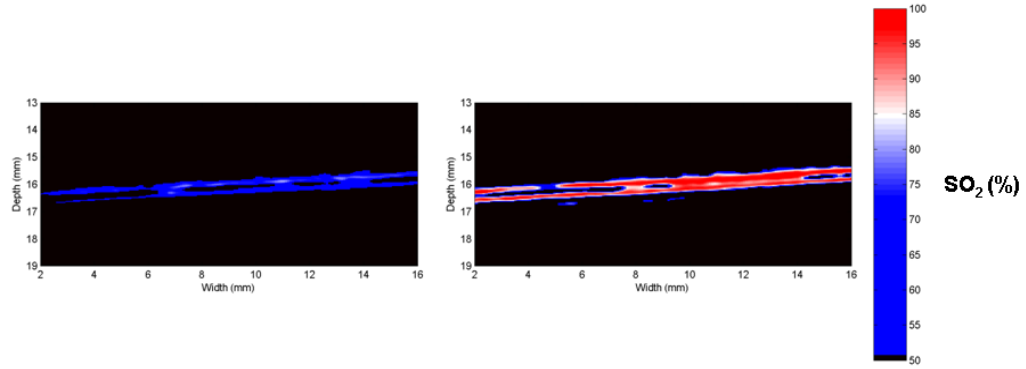

Figure 3: Oxygenation validation *ex vivo* experiment. Left: oxygen saturation map of a tube of venous blood drawn from a mouse breathing room air. Right: Oxygenation map of tube filled with venous blood drawn from same mouse 10 minutes after switching to 100% oxygen.

In Vivo Imaging of Murine Tumors

Subcutaneous tumors on the hind limb of nude mice were imaged with a variety of imaging modes on the Vevo 2100 system: B-Mode, PD Mode and the new PA Mode. B-Mode imaging gives structural information about the tumor and PD Mode maps the spatial distribution of blood flow. PA imaging can be presented as either a map of Total Hemoglobin Concentration (HbT) or Percentage Oxygen Saturation (SO_2). The ultrasound modes (B-Mode and PD Mode) are used as a means for correlating regions of blood flow within the tumor with the PA signals. PA imaging adds additional functional information (HbT and SO_2). Fig. 4 shows images from a representative image plane within a subcutaneous tumor. The PD image in Fig. 4a shows regions of flow within the tumor and can be overlaid on the B-Mode image (Fig. 4b). The PA image of total hemoglobin content, relative to the noise floor of the system (rHbT), shown in Fig. 4c is generated from a stack of twenty 2D images (spanning 2 mm). Each pixel in Fig. 4c reflects the maximum rHbT at the given location over the image stack and can also be overlaid on the B-Mode image to provide structural information (Fig. 4d). Finally, Fig. 4e presents a spatial map of percentage oxygen saturation (SO_2) which also can be overlaid with the B-Mode image (Fig. 4f). The images of SO_2 had a threshold applied which was based on the map of rHbT. All the images of rHbT and SO_2 were generated with a dual-wavelength measurement (700 and 800 nm). Differences between the PD Mode and PA images can be observed. This may be attributed to the improved sensitivity of PD Mode to vessels that are angled with respect to the transducer face, compared with the better

sensitivity of PA to structures that are parallel. In this respect, the two imaging techniques can be considered to be complementary. In general, Fig. 4 demonstrates the ability of the Vevo 2100 system to fuse functional information related to the distribution and oxygenation of blood, with structural information of cancerous tissue.

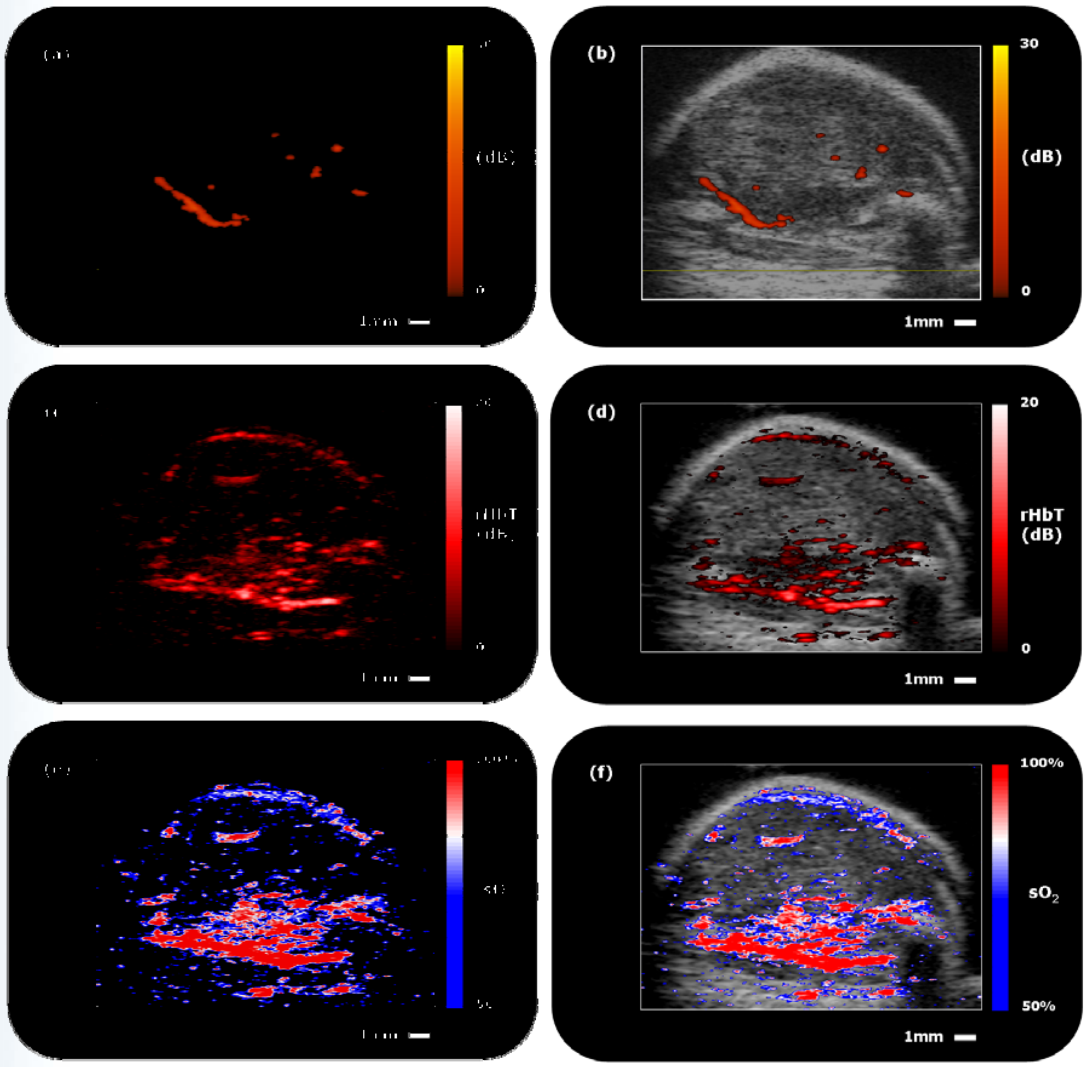

Figure 4: Functional images of blood flow in a subcutaneous tumor overlaid on B-Mode ultrasound images. Power Doppler Ultrasound images (a,b) show regions of blood flow within the tumor. Photoacoustic images of relative levels of Hemoglobin Concentration (rHbt) depict regions of blood flow not visible with Power Doppler (c,d). Photoacoustic images of Oxygenation Saturation (SO_2) provide additional functional information about the blood (e, f).

Future Directions for Photoacoustic Imaging

While the preliminary results for tumor imaging presented here show great promise, there are optimizations to signal and image processing that could be made to improve the quality of the PA images. Further validation will be performed to correlate the measurements of oxygen saturation with conventional techniques such as blood-gas analysis or histological staining. It should also be noted, that in order to increase the sensitivity and specificity of PA imaging, the use of contrast agents is warranted. Two types of contrast agents are available: Dye-based and nanoparticle-based. Dyes such as Indocyanine Green (ICG) and Methylene blue which are already being used in clinical procedures, have strong absorption in the near infrared. ICG can be introduced to the blood stream and enhance the inherent contrast of blood, resulting in better visibility of vasculature in deep tissue (Wang et al. 2004). Methylene blue that is injected under the skin will subsequently drain into the lymphatic system and accumulate in the Sentinel Lymph Node (SLN). Due to the strong contrast between the Methylene blue in the SLN and the surrounding tissue, the location of the SLN can be accurately identified in 3D using PA (Song et al. 2008). However, the scanning protocol offered by Song et al. requires scanning times of tens of minutes. Using the Vevo 2100 system, the protocol takes < 1 min.
Nanoparticles (NPs) exhibit stronger absorption of light than dyes and they can also be conjugated with antibodies and target specific cells expressing receptors indicative of a disease state, such as cancer. This has also led to their use for photothermal therapy, where they are exposed to ultrahigh light intensities, absorb the light, heat up and destroy the host tumor cells. Having the ability to image the concentration of NPs in the tumor area before the initiation of treatment is extremely advantageous. Several NPs are being used as contrast agents for PA. Carbon nanotubes conjugated with peptides were shown to enhance PA signal from tumors by eight times (De La Zerda 2008). Gold NPs have been delivered to tumors either by using targeting or using the enhanced permeability and retention of the tumor's leaky vasculature (Yang 2009).

Conclusions

PA imaging for preclinical research is anticipated to be a powerful imaging modality for the future. Recent developments on the Vevo 2100 micro-ultrasound platform allow for the integration of PA imaging that can be fused with B-Mode ultrasound. These images depict regions of blood flow and provide functional information of hemoglobin concentration and oxygen saturation of blood. Gathering this type of functional information is not possible with micro-ultrasound alone. PA imaging utilizes the optical absorption properties of blood and retains the image resolution and imaging depths of micro-ultrasound, something not possible with purely optical based imaging techniques. Finally, a variety of PA contrast agents exist which could be used to enhance the PA signal from blood or other tissue and cell types. The addition of PA to the Vevo 2100 system offers unique potential to add functional information on oxygenation to tumor studies using micro-ultrasound.

References

De La Zerda A et al 2008 Carbon nanotubes as photoacoustic molecular imaging agents in living mice *Nature Nanotechnol.* **3** 557–62

Ermilov SA, Khamapirad T, Conjusteau A, Leonard MH, Lacewell R, Mehta K, Miller T and Oraevsky AA 2009 Laser optoacoustic imaging system for detection of breast cancer *J. Biomed. Opt.* **14** 024007

Foster FS, Mehi J, Lukacs M, Hirson D, White C, Chaggares C, Needles A 2009 A new 15–50 MHz array-based micro-ultrasound scanner for preclinical imaging. *Ultrasound Med Biol*. **35** 1700-1708.

Kruger RA, Kiser WL Jr, Reinecke DR and Kruger GA 2003 Thermoacoustic computed tomography using a conventional linear transducer array. *Med Phys.* **30** 856-60.

Laufer J, Zhang E, Raivich G and Beard P 2009 Three-dimensional noninvasive imaging of the vasculature in the mouse brain using a high resolution photoacoustic scanner. *Appl Opt.* **48** D299-306.

Lungu GF, Li ML, Xie X, Wang LV and Stoica G 2007 In vivo imaging and characterization of hypoxia-induced neovascularization and tumor invasion. *Int J Oncol.* **30** 45-54.

Oraevsky A and Karabutov A 2003 Optoacoustic tomography Biomedical Photonics Handbook ed T Vo-Dinh (Boca Raton, FL: CRC Press)

Prahl S 1999 Optical Absorption of Hemoglobin http://omlc.ogi.edu/spectra/hemoglobin/

Siphanto RI, Thumma KK, Kolkman RG, van Leeuwen TG, de Mul FF, van Neck JW, van Adrichem LN and Steenbergen W 2005 Serial noninvasive photoacoustic imaging of neovascularization in tumor angiogenesis. *Opt. Express* **13** 89-95.

Song KH, Stein EW, Margenthaler JA and Wang LV 2008 Noninvasive photoacoustic identification of sentinel lymph nodes containing methylene blue in vivo in a rat model *J. Biomed. Opt.* **13** 054033–6

Wang L V and Wu H-i 2007 Biomedical Optics: Principles and Imaging (Hoboken, NJ: Wiley).

Wang XD, Pang Y J, Ku G, Xie X Y, Stoica G and Wang L H V 2003 Noninvasive laser-induced photoacoustic tomography for structural and functional in vivo imaging of the brain. *Nature Biotechnol*. **21** 803–6.

Wang XD, Ku G, Wegiel MA, Bornhop DJ, Stoica G, and Wang LV 2004 Noninvasive photoacoustic angiography of animal brains in vivo with near-infrared light and an optical contrast agent *Opt. Lett.* **29** 730-732.

Wang XD , Xie X Y, Ku G N and Wang L H V 2006 Noninvasive imaging of hemoglobin concentration and oxygenation in the rat brain using high-resolution photoacoustic tomography *J. Biomed. Opt*. **11** 024015.

Wang XD, Chamberland D L and Xi G H 2008 Noninvasive reflection mode photoacoustic imaging through infant skull toward imaging of neonatal brains *J. Neurosci. Methods* **168** 412–21.

Xiang L, Xing D, Gu H, Yang D, Yang S, Zeng L and Chen W R 2007 Real-time optoacoustic monitoring of vascular damage during photodynamic therapy treatment of tumor. *J Biomed. Opt.* **12** 014001.

Xu M H and Wang L H V 2006 Photoacoustic imaging in biomedicine *Rev. Sci. Instrum.* **77** 041101.

Yang X, Stein EW, Ashkenazi S and Lihong VW 2009 Nanoparticles for photoacoustic imaging. *Wire's Nanomed. and Nanobiotech.* **1** 360-368.

Zeng Y, Xing D, Wang Y, Yin B and Chen Q 2004 Photoacoustic and ultrasonic coimage with a linear transducer array. *Opt. Lett.* **29** 1760-1762.

Zhang H F, Maslov K, Stoica G and Wang L H V 2006 Functional photoacoustic microscopy for high-resolution and noninvasive in vivo imaging. *Nature Biotechnol.* **24** 848–51.

Glossary

Beamforming
The method used in array-based ultrasound to reconstruct an image from measured acoustic waves on the array elements. The method uses delay-and-sum algorithm.

A-Line
Historically, the first type of ultrasound scan derived from a single ultrasound pulse-echo line, updated as a function of time. The A-line would typically be displayed on an oscilloscope or similar display.

B-Mode
The traditional gray-scale ultrasound imaging mode derived from a series of ultrasound pulse-echo lines (see A-Lines), and shows structural information of organs and other tissues within a biological subject. The name "B-Mode" derives from historically coming after the term "A-Line".

Delay and sum
Technique where the arrival time of array signals is delayed based on the distance of the array element from the image point to be reconstructed, followed by summation of the delayed signals on all elements at the depth of the image point.

Extinction coefficient
Similar to absorption coefficient, only has units of $cm^{-1}M^{-1}$, and is therefore independent of concentration (M). Literature values for optical absorption are usually cited as extinction coefficient, since it is more generic and allows calculations for different concentrations.

Fluence
A measure of the concentration of light at a certain location. Fluence has units of energy per unit area and is most commonly expressed in mJ/cm^2.

Gruneisen parameter (Γ)
This parameter describes the efficiency with which heat converts into pressure during the process of thermo-elastic expansion, which underlies the photoacoustic effect. The Gruneisen parameter is different for different tissue types, but it usually varies in the range of 0.1-0.2 in soft tissue at body temperature.

Linear Array Transducer
An ultrasound transducer is a component that converts pressure into an electric signal. A linear array consists of 256 transducers packed closely along a line.

Optical Absorption coefficient (μ_a)
Optical absorption is the process where a photon (particle of light) is converted to a different form of energy, such as heat, potential or chemical energy. As a beam of light passes through tissue it gets attenuated exponentially due to absorption. The stronger the absorption, the faster the beam gets attenuated. The absorption coefficient describes the exponential coefficient and it is usually expressed in cm^{-1} or mm^{-1}. An

absorption coefficient of 1 cm^{-1} means that light passing through 1 cm of tissue comes out with 1/e of the initial intensity.

Optical Parametric Oscillator (OPO)
An optical module used to convert laser wavelength to a higher wavelength. Its primary advantage is the ability to tune the final wavelength within quite a broad range. For instance, the laser used in this study has an OPO that produces wavelengths in the range of 680-950 nm.

Oxygen saturation (SO_2)
Hemoglobin, the red blood cell protein that carries oxygen in the blood stream, can bind up to four oxygen molecules. As can be seen in fig. 2, the optical absorption spectrum of hemoglobin changes drastically as it changes its state from fully oxygenated (HbO_2) to entirely oxygen-free (Hb). The oxygen saturation metric, expressed as percentage, describes the average oxygenation state of the hemoglobin molecules at the site of measurement.

Power Doppler
A well established ultrasound imaging mode which uses signal processing estimates to determine regions of blood blow within soft tissue and displays the detected signal as a color overlay on B-Mode ultrasound images.

Quadrant
A subset of the array comprising 64 elements. Q1 includes elements 1-64, Q2 includes elements 65-128 and so forth.

Repetition rate
The number of times the laser fires per second.

VISUALSONICS

VisualSonics
T. +1.416.484.5000
E. info@visualsonics.com
W. www.visualsonics.com

Authors: Pinhas Ephrat, Andrew Needles, Corina Bilan, Anna Trujillo, Catherine Theodoropoulos, Desmond Hirson, Stuart Foster